Global and Planetary Change 92–93 (2012) 257–266

Contents lists available at SciVerse ScienceDirect

Global and Planetary Change

journal homepage: www.elsevier.com/locate/gloplacha

A 300-year history of Pacific Northwest windstorms inferred from tree rings

Paul A. Knapp [a,*], Keith S. Hadley [b]

[a] Carolina Tree-Ring Science Laboratory, Department of Geography, University of North Carolina, Greensboro, NC, USA
[b] Geography Department, Portland State University, Portland, OR, USA

ARTICLE INFO

Article history:
Received 16 March 2012
Accepted 5 June 2012
Available online 13 June 2012

Keywords:
Pacific Northwest
Windstorms
Sitka spruce
Tree rings
Climatic indices

ABSTRACT

Hurricane-force winds are frequently allied with mid-latitude cyclones yet little is known about their historical timing and geographic extent over multiple centuries. This research addresses these issues by extending the historical record of major mid-latitude windstorms along North America's Pacific Northwest (PNW) coast using tree-ring data collected from old-growth (>350 years), wind-snapped trees sampled at seven coastal sites in Oregon, USA. Our objectives were to: 1) characterize historical windstorm regimes; 2) determine the relationship between high-wind events (HWEs) and phases of the PDO, ENSO and NPI; and 3) test the hypothesis that PNW HWEs have migrated northward. We based our study on the identification of tree-growth anomalies resulting from windstorm-induced canopy changes corresponding to documented (1880–2003) and projected HWEs (1701–1880). Our methods identified all major windstorm events recorded since the late 1800s and confirmed that variations in coastal tree-growth are weakly related to temperature, precipitation, and drought, but are significantly related to peak wind speeds. These results suggest wind-induced changes in canopy conditions control tree growth at all sites. Comparisons between the tree-ring record and the PDO, NPI, and ENSO revealed a significant positive correlation between HWEs and neutral to warm PDO conditions and a slightly weaker correlation with the NPI. ENSO events were not significantly related to the occurrence of HWEs. Latitudinal groupings of our sites revealed a gradual and non-significant northerly shift of HWEs until the late 19th century followed by a significant northward shift during the past 120 years. These results mark the application of dendroanemology as a method for characterizing windstorm regimes for multiple centuries.

1. Introduction

Hurricane-force winds derived from East Pacific mid-latitude cyclones and typhoon remnants are common events along North America's Pacific Northwest (PNW) coast occurring at a similar or higher frequency than those experienced by the most hurricane-prone regions of the U.S. Atlantic and Gulf Coasts (Keim et al., 2007; Mass and Dotson, 2010; Hadley and Knapp, 2011). With documented winds gusts to 179 kt (Mass and Dotson, 2010), these high-wind events (HWEs) exert a regional-scale influence on the economy (Decker et al., 1962) causing extensive property damage (e.g., Reed, 1980), prolonged regional-scale power outages (Read, 2011), and severe disturbance to coastal and Coast Range forests (Ruth and Yoder, 1953). HWE property damage and loss in Oregon and Washington from 1950 to 2009 has been conservatively estimated to be between $10 and 20 billion (Mass and Dotson, 2010) with an average PNW region loss of $112 million per event during 1952–2006 (Changnon, 2009). These windstorms represent the only form of severe weather in the United States that is most pronounced on the West Coast (Changnon, 2009).

Similar to the role of fire in drier climates, HWEs are arguably the single-most important disturbance agent shaping the PNW's marine west coast forests (Kirk and Franklin, 1992; Hadley and Knapp, 2011) with at least five HWEs having caused forest blowdowns exceeding 1 billion board feet (>2.36 million m³) since 1880 (Read, 2011). As Read (2011) notes: "No hurricane in history, no matter how strong, managed to knock down as much forest as the great gale [i.e., Columbus Day Storm] of 1962." In addition to the economic losses associated with forest blowdown, these regional windstorms create a range of canopy conditions that shape ecological succession, forest structure (Franklin et al., 2002; Harcombe et al., 2004), and create large fuel loads that may have contributed to the infrequent but intense fires that have historically affected the western PNW (Weisberg and Swanson, 2003).

Despite the growing recognition of PNW windstorms as major climatic events (Read, 2011), HWEs have received little public or research attention relative to their eastern North America counterparts because of the region's lower population density and because the majority of wind-related damage reflects a loss of forest resources rather than human-built features (Mass and Dotson, 2010). Consequently, little is known about their timing, extent, and causes over periods spanning decades to centuries relative to the documented and pre-instrumental history of Atlantic hurricanes (e.g., Liu and Fearn, 1993, 2000; Donnelly et al., 2001; Donnelly and Woodruff, 2007; Nyberg et al., 2007). By

* Corresponding author at: Carolina Tree-Ring Science Laboratory, Department of Geography, University of North Carolina-Greensboro, Greensboro, NC 27402, USA.
E-mail address: paknapp@uncg.edu (P.A. Knapp).

0921-8181/$ – see front matter © 2012 Elsevier B.V. All rights reserved.
doi:10.1016/j.gloplacha.2012.06.002

comparison, detailed records of Pacific Coast windstorms are sparse before 1950 with few quantitative measures of storm activity before this date. This limits our knowledge of the occurrence and severity of pre-1950 windstorms to qualitative accounts derived from newspaper articles, historic photographs, data logs (Read, 2011), and journal entries (Knapp and Hadley, 2011).

Pacific Northwest windstorms rival their North Atlantic counterparts in several ways. Central low pressures of PNW mid-latitude cyclones can drop below 960 mb (Reed and Albright, 1986; Mass and Dotson, 2010) meeting the criteria of category-3 hurricanes. Sustained wind speeds generated by these storms have reached 130 kt (Mass and Dotson, 2010) with multiple sites recording sustained winds over 83 kt matching those of category 2–3 hurricanes. These storms are further accompanied by heavy rains, flooding and storm surges (Read, 2011). Mid-latitude cyclones creating HWEs in the PNW tend to be larger and generate higher inland wind speeds than most Atlantic hurricanes. Several storms, including the Columbus Day Storm (CDS) of 1962, have generated wind speeds > 87 kt at sites located 80 km inland from the coast including portions of the heavily populated Willamette Valley and Puget Sound region (Lynott and Cramer, 1966; Read, 2011).

Despite their role as a pervasive disturbance agent to regional ecosystems and their hazard to local and regional communities, there are no centennial-length or longer records that describe the frequency of PNW windstorms. Relevant questions concerning these events include how often and how severe were these windstorms in the past (e.g., Knapp and Hadley, 2011) and what is their future role in a region experiencing rapid development? Is windstorm frequency related to sub-decadal (ENSO) and decadal (PDO) climate oscillations and warmer or cooler oceanic temperatures that affect the synoptic climatology of the PNW? For example, Enloe et al. (2004) found that monthly peak wind gusts and frequency of gale-force winds increased (decreased) during La Niña (El Niño) phases throughout the winter months in the PNW during the latter half of the 20th century. Similarly, Chen and Yoon (2002) discussed how the PDO modulates the strength of the Aleutian Low and its effects on cyclogenesis and storm-track trajectories in the PNW. Finally, what are the social, economic, and ecological implications of these storms in an increasingly warmer world?

Our research seeks to address these questions by extending the record of major windstorms to the early 1700 s using tree-ring data collected from old-growth trees located along Oregon's PNW coast. Our general objective is to place severe windstorm events in a broader historical context that better defines the range of variability of PNW HWEs. More specifically, we seek to: 1) identify the timing and relative magnitude of these windstorms; 2) describe their spatial and temporal variation; 3) determine their temporal correlation with phases of the PDO and ENSO; and 4) test the hypothesis that HWEs in the Pacific Northwest have migrated northward over the last century (cf. Mass and Dotson, 2010). Answers to these questions would provide several public and scientific benefits including a historical basis for estimating the probability and severity of current and future HWEs, assessing the role of HWEs on the regional ecology and economy, and aiding agency preparedness.

2. Methods

Tree-ring data for this research were collected from wind-snapped, old-growth (>350 years) Sitka spruce (*Picea sitchensis*) (four sites) and Douglas-fir (*Pseudotsuga menziesii*) (three sites) trees located in five state parks and two Research Natural Areas along the Oregon Coast (Fig. 1). Both of our target tree species are large diameter (>2–4 m), long-lived (>500 years), and fast-growing in the PNW (Waring and Franklin, 1979). These species can attain a mean height of ca. 50 m within the first 100-years of growth along the Oregon Coast (Waring and Franklin, 1979; Harris, 1990) making them susceptible to both windsnap and episodes of accelerated growth (ecological release). In all instances, our sample sites were selected for their

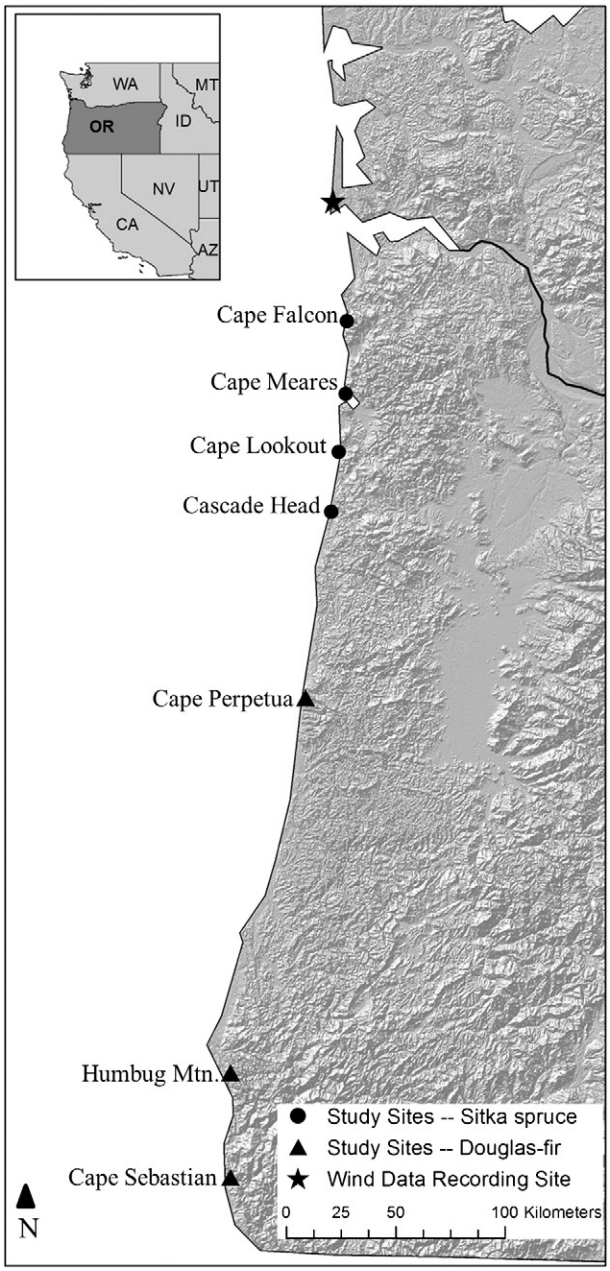

Fig. 1. Location of the seven study sites along the Oregon coast and the wind data recording site in North Head, Washington. Sitka spruce trees were sampled at the four northern study sites and Douglas-fir trees were sampled at the three southern study sites.

abundance of old-growth trees and exposure to windstorms. Wind-snapped trees were visually identified in the field as live trees lacking an upper bole and displaying post-traumatic canopy replacement by apical branch growth (Fig. 2). We sampled 13 to 33 trees (26–63 cores) at each site, collecting two 60–76 cm length cores from each tree at approximately 1.4 m height.

Following removal, all cores were prepared for ring-width measurements using standard procedures (Stokes and Smiley, 1968; Speer, 2010) and visually crossdated using the list method (Yamaguchi, 1991) as a preliminary procedure to ensure dating accuracy. Each ring in each of the visually crossdated cores was then measured to the nearest 0.001 mm using binocular microscopes in conjunction with VELMEX sliding measuring benches. Ring-width measurements for each core were then statistically crossdated using the program COFECHA (Holmes, 1983) to ensure dating accuracy (Grissino-Mayer, 2001; Speer, 2010). All potential problem segments identified using

Fig. 2. Wind-snapped Sitka spruce at Cape Meares State Park, Oregon. Loss of the upper portion of central bole is often compensated by extensive growth to upper branches—"muscle arms"—that mitigate windstorm-induced canopy loss and long-term growth reduction in coastal trees.

COFECHA were reexamined to ensure crossdating accuracy per standard dendrochronology protocol (Grissino-Mayer, 2001; Speer, 2010). A total of 61% of the trees (51% of the cores) were successfully crossdated. A post-hoc examination of unsuccessfully crossdated cores revealed that these cores typically included multiple missing rings consistent with severe canopy trauma following severe HWEs. Cores with confirmed dating accuracy were then standardized to create dimensionless index values using the program ARSTAN (Cook, 2005). This procedure applied a 30-year cubic spline to each ring-width series to eliminate age-related growth trends associated with increases in tree diameter while retaining high-frequency variance (Cook and Holmes, 1986; Grissino-Mayer, 2001). This procedure was repeated for all visually and statistically crossdated cores for each of the seven sample sites. Upon completion, continuous data for the seven sites were available from 1701 to 2008 (Table 1).

Following methods presented in Hadley and Knapp (2011) we detected HWEs by identifying growth suppressions associated with windsnap (traumatic canopy loss) and growth releases resulting from tree-canopy openings caused by windthrow and canopy breakage of adjacent trees. We used tree-ring index values deviating from the mean by $\leq$50% (representing growth suppressions) or $\geq$50% (representing growth releases) for each core to identify HWEs. This approach, based on total standardized chronology length, is similar to the boundary-line method proposed by Black and Abrams (2003) that includes prior radial-growth as a predictor of maximum-growth change following disturbance. This method provides a conservative estimate of HWEs based on the occurrence of radial growth anomalies similar to that used by dendroecologists to identify insect outbreaks and fire years (e.g., Speer et al., 2001; Arabas et al., 2006). The use of standardized chronologies also allowed us to compare individual cores for all years while retaining 99% of the high-frequency radial-growth variation during a 9.3-year cycle (Hadley and Knapp, 2011). Earlier research along the Oregon coast has shown monthly climatic variables are poorly associated with tree growth (Knapp and Hadley, 2011) and that other growth-altering factors such as disease, fire, and snow/ice storms are uncommon along the coast and unlikely to contribute to significant growth variations across the region (Hadley and Knapp, 2011).

We designated HWE years at each site when $\geq$15% of the cores (minimum of 3–5 cores) met the $\pm$50% growth deviation threshold. Experimentation with lower and higher thresholds revealed the 15% criterion best captured storm frequency and magnitude and successfully identified ca. 80% of the 20th century windstorms at Cape Falcon (Hadley and Knapp, 2011). Comparison of the 15% threshold with absolute percentages of growth anomalies revealed the 15% threshold produced a better unbiased (i.e., not sample-size related) replication of the documented windstorm history (Fig. 3). We ended our analysis in 2003 to avoid sample bias related to a recent period of high windstorm frequency during 2004–2008 (Read, 2011).

We examined the temporal correlation between the occurrence of HWEs and the Pacific Decadal Oscillation (PDO) by comparing averaged monthly PDO values for October of the previous year through the following January with the annual total of current-year growth anomalies exceeding the 15% threshold from 1925 to 2003 (http://jisao.washington.edu/pdo/) for all seven sites. This allowed us to compare a four-month average of PDO conditions with tree-ring data derived for the same year with PDO years identified by index values as warm ($>$0.5), cold ($<-$0.5), or neutral phases (between 0.5 and $-$0.5). We selected 1925 as the beginning year of our comparison as it marked the onset of a well-defined warm-phase of the PDO (Mantua et al., 1997) and because of the relative paucity in Pacific Ocean recording stations during the early 1900s (cf. Biondi et al., 2001; MacDonald and Case, 2005). We then calculated 5-year running averages for PDO data to mitigate the potential lag effects between HWEs and growth responses and to compensate for the seasonal variations associated with early-season (October through January) and late-season (February

Table 1
Summary statistics for the seven site chronologies. Sites are listed from northernmost (Cape Falcon) to southernmost (Cape Sebastian).

	Cape Falcon	Cape Meares	Cape Lookout	Cascade Head	Cape Perpetua	Humbug Mountain	Cape Sebastian
Number of dated trees	18	16	16	8	17	14	19
Number of dated series	29	26	22	16	33	24	35
Master series (years)	427	348	308	439	407	458	333
Total rings in all series	8871	5608	4669	3373	8894	6938	8304
Total dated rings checked	8860	5535	4651	3372	8878	6839	8297
Series intercorrelation	0.419	0.426	0.397	0.439	0.544	0.554	0.51
Average mean sensitivity	0.225	0.25	0.231	0.241	0.229	0.224	0.261
Segments: possible problems	84	54	63	33	26	26	25
Mean length of series (years)	305.9	215.7	212.2	210.8	269.5	289.1	237.3
Chronology period	1508–2007	1661–2008	1701–2008	1570–2008	1602–2008	1550–2007	1676–2008
Sample # Cores (Begin/End)	17/28	1/19	1/18	4/16	14/33	11/24	5/29

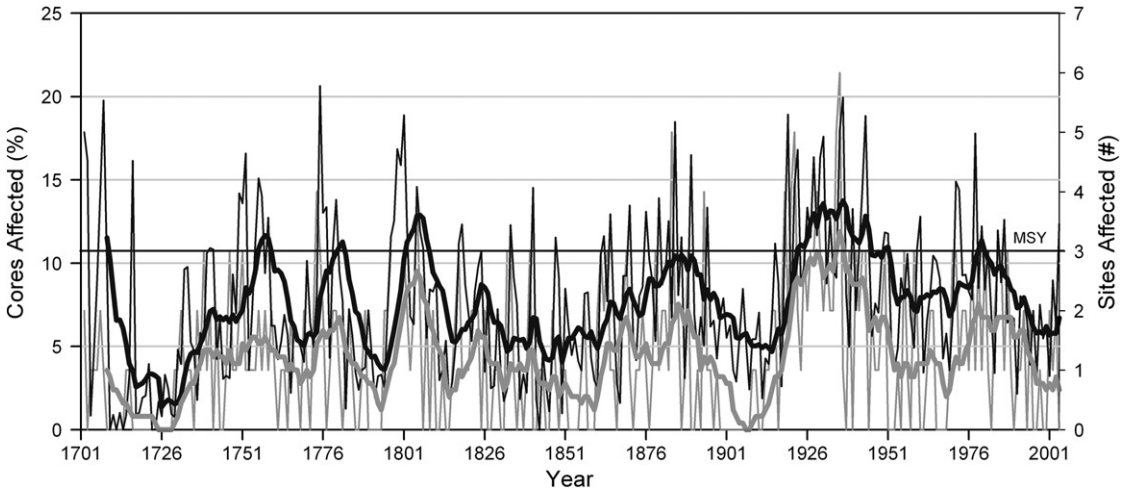

Fig. 3. Percentage of tree-ring cores meeting the ±50% growth deviation threshold for all sites combined (black) and the annual number of sites that recorded a HWE (gray). Ten-year running means are shown as bold lines. The horizontal black line identifies the major storm year (MSY) threshold, i.e., years having HWEs recorded at ≥3 sites.

through April) HWEs. This procedure mitigated the longer-term effects of HWEs on radial growth and more closely approximated the low-frequency change in the PDO index relative to those of ENSO and NPI. Experimentation revealed that a 5-year period produced a stronger correlation than shorter periods; longer periods yielded nominal increases in r values. These smoothed differences in interannual variability were then correlated with the 5-year running means of HWEs. We adjusted for autocorrelations and non-normality in the PDO and smoothed HWE data by calculating "effective" degrees of freedom using the procedures described in Garrett and Petrie (1981). We used superposed epoch analysis (SEA; e.g., Grissino-Mayer and Swetnam, 2000; Heyerdahl et al., 2002) to provide a nonparametric comparator of our correlation results. This analysis compared PDO index values and HWEs using lagged (±5 years) and current-year data. Events were defined as years with ≥1 HWE and ≥3 HWEs (i.e., major storm years).

We examined two additional indices to determine the correlation between HWEs and the potential influence of other known climate oscillations. First, we compared ENSO data based on average (July–Nov) SOI values (WRCC, 2010) to tree-ring indices representing the following growing season (i.e., July–Nov 2002 SOI matched with 2003 ring width). The ENSO data extend from the winter of 1933–34, the beginning of continuous monthly SOI values (Redmond and Koch, 1991), through the winter of 2002–2003. These values were then classified as strong El Niño, moderate El Niño, Neither (i.e., neutral), moderate La Niña, or strong La Niña following the criteria of Redmond and Koch (1991). We then compared the 1925–2003 annual values of the North Pacific Index (NPI) to the number of HWEs. NPI is a measure of atmospheric circulation as denoted by mean sea-level pressure for the region 30–65° N and 160° E–140° W (Trenberth and Hurrell, 1994). We chose the mean of October–January values using 1925 as the initial year of analysis because of the lower reliability of sea-level pressure data during the earlier (1899–1924) portions of the data set (Trenberth and Hurrell, 1994) and to be temporally consistent with our PDO analyses. Examination of the potential relationships between monthly and seasonal PNA indices with our HWE record revealed no significant correlations ($p > 0.05$) during the period of available data (1950–2003) (CPC, 2012) and was excluded from further analysis.

The spatial extent of HWEs were determined by identifying years having ≥3 of the seven tree-ring collection sites recording an event during 1701–2003. Years meeting these criteria ($n = 48$) were designated as Major Storm Years (MSYs) and were used to identify HWEs that tracked parallel to the Oregon Coastline affecting sites across a large latitudinal extent. These storms were more likely to be recorded by the tree-ring record at multiple sites than storms that tracked inland following landfall. Using these criteria, our method identifies MSYs in terms of storm strength (i.e., >15% cores affected at a site) and geographical extent (i.e., number of sites affected).

The geographic distribution of each MSY was determined using a two-part procedure. First, we assigned the geographic location of each MSY to one of three categories: 1) "North" (Cape Falcon, Cape Meares and Cape Lookout), 2) "Central" (Cascade Head and Cape Perpetua), and 3) "South" (Humbug Mountain and Cape Sebastian) (Fig. 1). The resulting classifications of MSYs included tree-ring evidence of a HWE in any one or any combination of geographic categories. We used Chi-square comparisons of MSYs between the 18th, 19th, and 20th (i.e., 1900–2003) centuries to identify significant temporal changes in their geographic occurrence. Second, we determined the mean geographic locations of MSYs by averaging the latitude of each site recording a HWE in a given year. We then applied regression analyses to determine if MSYs (independent variable) varied with mean latitude (dependent variable) over time. We identified outliers as years having standardized residuals >2.5 and used the Durbin-Watson test (Zar, 1999) to identify potential serial autocorrelation.

Monthly temperature, precipitation and Palmer Drought Sensitivity (PDSI) data from Oregon Climate Division 1 (Coastal) were used as independent variables to develop growth/climate regression models for each chronology (NCDC, 2010). We used radial growth as the dependent variable and stepwise regression to obtain the best models during 1895–2003.

Wind speed and growth-anomaly comparisons were made using maximum wind velocity data collected at North Head, Washington from 1914 through 1949 (MWR, 1914–1949) and the annual number of sites recording a HWEs our central to northern Oregon coast sites (i.e., Cape Perpetua to Cape Falcon). North Head, located ca. 65 km north of Cape Falcon and 240 km north of Cape Perpetua (Fig. 1), is the closest coastal wind recording station near our sample sites with long-term, continuous monthly wind speed records. Record length was based on the beginning and ending of an active phase of HWEs along the central to northern Oregon coast that coincided with a continuous and available wind-data record from the North Head station. Peak wind speed was determined using a 1.3 multiplier on 1-minute (or longer) maximum wind speeds (Read, 2011) after adjusting 4-cup anemometer data recorded from 1914 to 1927 (MWR, 1894:29).

3. Results

3.1. Tree-growth–climate relationships

Tree-growth correlations with climate variables for the seven sites ranged from an R^2 value of 0.24 at Cape Falcon to non-significant at

Table 2
MSYs identified by date and geographical centroid location (north to south) along the Oregon Coast. N = north coast (Cape Falcon, Cape Meares and Cape Lookout); C = central coast (Cascade Head and Cape Perpetua); S = south coast (Humbug Mountain and Cape Sebastian). NNN indicates a MSY identified at the three northern sites. CCS indicates a MSY at two central sites and one southern site. Median dates of events by location are shown in far right column.

Location	Year	Year	Year	Year	Year	Year	Year	Year	Year	Year	Year	Year	Median Date
NNN	1926	1929											1928
NNNCS	1934												1934
NNNCCS	1935												1935
NNNS	1928												1928
NNC	1833	1861	1878	1924	1940	1942	1949	1958	1970	1980	1984	1987	1946
NNCS	1804												1804
NNS	1796	1800	1869	1938	1976	1978							1904
NCC	1750	1832											1791
NNCSS	1920	1921											1921
NNSS	1893												1893
NCS	1738	1746	1774	1797	1798	1799	1863	1888	1927	1943	1955	1971	1831
NCCS	1773												1773
NCSS	1918												1918
NCCSS	1883												1883
NSS	1817	1931											1874
CCS	1839	1985											1912

Cape Perpetua (Table 3). The remaining sites yielded R^2 values between 0.13 and 0.06. Summer temperature or summer temperature and September precipitation combined, were significant growth variables at the four northernmost sites (Table 3). A less-defined pattern was present for the three southernmost sites (Table 3).

The annual number of sites recording a HWE at the five central to northern sites were significantly correlated ($r_s = 0.403$, $p = 0.016$, $n = 35$) with peak wind gusts at North Head despite distance to the climate station (Table 4). The majority of peak gusts for each winter (O–A) occurred in December and January (Table 4). Data from 1920 were excluded as an outlier as peak wind speed at North Head was low compared to the number of sites affected and maximum wind speed occurred in January. Weidman (1920: 837), however, notes that a "destructive" windstorm "prevailed over most of the Northwest" on April first and second and this storm may have been responsible for the HWE recordings at multiple sites (Table 4). The peak wind gust of 106.5 kph from the NW recorded on April 2nd at North Head is modest, but the direction is consistent with the type of powerful windstorms noted in Read (2011) and identified as "Class 2 Events." These wind storms track inland between the central Oregon to southern Washington coastline with diminished wind speeds at locations north of the low (i.e., locations experiencing NW winds) such as occurred at North Head on this date.

3.2. Temporal activity of HWEs/MSYs

Based on 8–19 crossdated trees (median = 17) from each site (Table 1), we identified episodic HWE activity over the 303-year study period with 0–6 sites experiencing a HWE in a given year (Fig. 4). The earliest recorded event occurred in 1701 and the most recent in 2002. Core sample depths for all sites ranged from 53 in 1701, 180 in 1920 and 167 in 2003 (Fig. 4, Table 1). There were a total of 372 HWEs recorded over the study period at the seven sites with an average of 1.23 HWEs/year. Using the MSY threshold filter where ≥3 sites recorded a HWE in a given year, we identified three periods of above-average activity: 1796–1800, 1918–1943, and 1970–1987 (Fig. 3). Notable non-active phases included the periods of 1806–1831, 1840–1860, 1894–1917 and 1959–1969 (Fig. 3). The single most extensive events occurred in 1934 and 1935 where 5 and 6 sites, respectively, recorded HWEs. Five sites recorded activity in 1921 and 1883, and four sites recorded HWEs in 1773, 1893, 1918, 1920 and 1928. The longest periods without HWEs were 1716–1728 and 1898–1907. The 48 MSYs represented 15.8% of the total record with a mean return interval (MRI) of 6.31 years. By century, ten (21%) of the MSYs occurred during 1701–1800, 12 (25%) occurred during 1801–1900, and 26 (54%) occurred during 1901–2003. During the 20th century, 15 MSYs were clustered into a 26-year period between 1918 and 1943 with a mean return interval of 1.7 years; no MSYs were identified during 1701–1737, 1775–1795, 1840–1860, 1894–1917 and 1988–2003.

3.3. PDO–HWE interactions 1925–2003

A total of 22 MSYs were identified, with 11 occurring during warm years, 8 occurring during neutral years, and 3 occurring during cold years. The frequency of HWEs is positively and significantly correlated with Nov–Jan PDO conditions (Fig. 5). Between 1925 and 2003 ($n = 79$ years), periods of elevated storm activity were associated with warm or neutral PDO conditions with the highest correlation ($r = 0.344$, $p = 0.05$, $df_{adj} = 31$) derived using 5-year running mean values of HWEs and PDO values. During this period, there were 20 warm, 34 neutral, and 25 cold PDO years (Fig. 5). Mean PDO index values of MSYs ($n = 22$, $\bar{x} = 0.248$) were significantly higher ($p = 0.035$, 1-tailed Mann–Whitney) than non-MSYs ($n = 57$, $\bar{x} = -0.227$). There was no significant relationship ($p > 0.05$) between annual PDO and HWE values.

Results of our SEA between PDO index values and MSYs (≥3 sites) revealed a positive 1-year lag with MSYs ($p < 0.05$) indicating tree-ring growth anomalies during major storm years were preceded by warmer-phase PDO conditions. These results are consistent with our

Table 3
Results of growth/climate models for seven sampling sites. Locations are listed from north to south. No climate variables were significant at $\alpha = 0.05$ for the Cape Perpetua model.

Site	R^2	p	Equation
Cape Falcon	0.24	<0.000	Radial growth = 2.868 − 0.032 (June Temperature) + 0.022(Prior-year October PDSI)-0.019(September Precipitation)
Cape Meares	0.11	0.002	Radial growth = 2.678 − 0.033 (April Temperature) − 0.026(September Precipitation)
Cape Lookout	0.09	0.008	Radial growth = 2.651 − 0.022 (September Precipitation) − 0.027(July Temperature)
Cascade Head	0.06	0.011	Radial growth = 2.989 − 0.033 (July Temperature)
Cape Perpetua	NA	NA	NA
Humbug Mountain	0.06	0.013	Radial growth = 1.005 + 0.02 (July PDSI)
Cape Sebastian	0.13	0.001	Radial growth = 2.929 − 0.36 (Prior-Year October Temperature) − 0.021(January PDSI)

Table 4
Number of sites along the central to northern Oregon coast (Cape Falcon, Cape Meares, Cape Lookout, Cascade Head, and Cape Perpetua) affected by HWEs during 1914–1949 with associated wind speeds and estimated peak gusts at North Head, Washington based on wintertime (previous year O–D and current-year J–A) data. Wind speeds represent the highest value for each winter with month of occurrence listed.

Year	Number of sites recording a HWE	Recorded wind speed at North Head (kph)	Estimated peak wind speed at North Head (kph)	Month of maximum wind speed
1914	1	113.6	147.7	Jan
1915	1	104.6	136.0	Nov
1916	0	115.8	150.6	Jan
1917	2	119.4	155.2	Dec
1918	2	104.6	136.0	Dec
1919	1	109.1	141.8	Jan
1920	3	93.3	121.3	Jan
1921	3	139.5	181.8	Jan
1922	2	111.3	144.7	Dec
1923	1	104.6	136.0	Jan
1924	3	109.1	141.8	Dec
1925	2	104.6	136.0	Feb
1926	3	113.6	147.7	Nov
1927	2	117.0	152.1	Dec
1928	3	125.5	163.2	Oct
1929	3	115.8	150.6	Dec
1930	2	115.8	150.6	Feb
1931	1	99.8	129.7	Jan
1932	2	115.8	150.6	Dec
1933	2	127.1	165.2	Dec
1934	4	112.6	146.4	Dec
1935	5	140.0	182.0	Oct
1936	0	117.5	152.7	Jan
1937	0	112.6	146.4	Feb
1938	2	115.8	150.6	Nov
1939	0	107.8	140.1	Dec
1940	3	127.1	165.2	Dec
1941	2	135.2	175.7	Dec
1942	3	107.8	140.1	Dec
1943	2	123.9	161.1	Apr
1944	0	104.6	136.0	Dec
1945	2	104.6	136.0	Dec
1946	1	107.8	140.1	Jan
1947	1	106.2	138.1	Jan
1948	2	111.0	144.3	Feb
1949	3	111.0	144.3	Feb

presumed post-disturbance growth lag and the time gap between HWE season (previous-year October–April) and the following spring-fall growing season. Conversely, SEA failed to reveal a significant relationship for PDO index values and HWEs occurring at ≥1 site(s) suggesting different event criteria may reflect the importance of local topography or that specific site conditions become less important during large-scale or regional events.

3.4. ENSO– and NPI–HWE interactions

There were 17 MSYs during the 70-year period with SOI values (1934–2003). Of these, two MSYs occurred during strong and three during moderate El Niño years, ten during neutral years, one during moderate La Niña years, and one during a strong La Niña year. The percentages of MSYs relative to the frequency of ENSO events indicates that 5 of 21 (24%) of El Niño years experienced a MSY while 2 of 14 (14%) La Niña years coincided with a MSY. Ten of 34 (29%) neutral ENSO conditions were associated with MSYs. Mean SOI values of MSYs ($n=17$, $\bar{x}=-0.175$) were not significantly different ($p=0.316$, 1-tailed Mann–Whitney) than non-MSYs ($n=53$, $\bar{x}=-0.133$). Despite the better match with neutral ENSO conditions we found no significant correlation between annual ENSO index values and HWEs ($r_s=-0.110$, $p=0.365$). Winter (October–January) NPI values (1925–2003) were significantly and negatively correlated with HWE activity using annual data ($r_s=-0.238$, $p=0.035$). Mean NPI values for MSYs ($n=22$, $\bar{x}=1008.70$ mb) were significantly lower ($p=0.021$, 1-tailed Mann–Whitney) than non-MSYs ($n=57$, $\bar{x}=1009.63$ mb).

3.5. Spatial components

Twenty MSYs were concurrently recorded in all three regions (North, Central, South), suggesting that 43% of these storms traveled parallel to the coastline (Table 2) or were regional in scale. Tree-ring evidence of other HWEs indicates the majority were sub-regional in extent. Sixteen MSYs were recorded in the North or Central regions, but not the South, 12 MSYs were detected in the North and South, but not the Central, and two MSYs did not occur in the Northern sites (Table 2). The spatial distribution of storm tracks also appeared to change by century. During 1701–1800, 90% (9 of the 10) MSYs were represented by HWEs recorded in both North and South sub regions decreasing to 67% (8 of 12) from 1801 to 1900, and to 58% (15 of 26) between 1900 and 2003 (Table 2). Chi-square comparisons among centuries showed differences at $\alpha<0.10$ between the 1701 and 1901 periods (Yate's $p=0.064$, one-tailed), and between the 1701 and the combined 1801–1901 periods (Yate's $p=0.075$; one-tailed). These results correspond to a lower frequency of MSYs along the southern Oregon coastline and an increase in MSYs along the North and Central coast beginning during the late 19th century.

Examination of standardized residuals generated from the regression model (i.e., mean geographic position of HWEs and date) indicated that MSY 1985 was an outlier with a southerly mean position. Removing this year from our data ($n=47$ MSYs) yielded a weak but significant spatio-temporal relationship when using linear regression ($R^2=0.122$, $p=0.016$) and a 2nd order polynomial ($R^2=0.137$, $p=0.039$) (Fig. 6). Prior to the late 19th century, there was minimal northward migration in the mean geographic position of HWEs during MSYs, but a significant ($R^2=0.18$, $p=0.025$, $n=28$) northward migration occurred from 1883 onward.

4. Discussion

4.1. Detection of major windstorms

Earlier methodologically based research has demonstrated the utility of tree-ring data to accurately detect HWEs along the Oregon coast using two geographically separated sites (Hadley and Knapp, 2011) during 1895–2003. The results reported here incorporate data for five additional sites successfully identifying most of the historically-documented MSYs along the Oregon Coast including those of 1883 (storm on 2 October 1882; Read, 2011), 1920 (2 April 1920; Weidman, 1920), 1921 (29 January 1921; Read, 2011), and 1935 (21 October 1934; Read, 2011). No MSYs were falsely identified—we did not detect any undocumented HWEs during the historical period of record. We also found that the number of HWEs is significantly and positively correlated with wind speed indicating the growth anomalies we detected in our tree-ring data are consistent with peak wind velocity.

4.2. Temporal activity of HWEs/MSYs

The temporal activity of HWEs is marked by a multi-decadal periodicity of higher and lower activity significantly correlated with phase oscillations of the PDO. These findings suggest: 1) growth anomalies identifying discrete events (i.e., HWEs) can be used to identify PDO years, and 2) neutral to warm PDO conditions are positively correlated with HWEs. These results are statistically weaker but consistent with other North American, West Coast tree-ring reconstructions based on cool-season precipitation (e.g., Biondi et al., 2001; D'Arrigo et al., 2001; Gedalof and Smith, 2001).

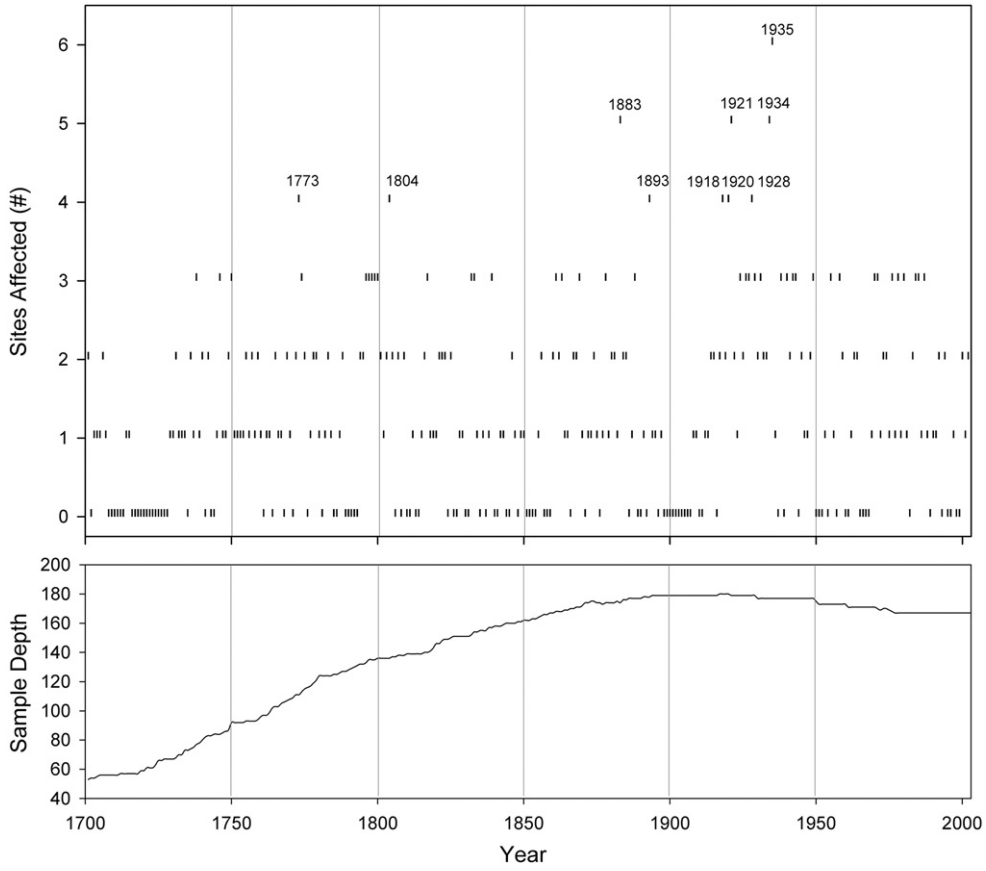

Fig. 4. Number of sites ($n=7$) annually affected by a HWE: 1701–2003. Years with notable windstorms are labeled. Zero values represent years when no site recorded a HWE. Vertical lines representing 50-year intervals added for visual comparisons. Lower graph presents sample depth (number of cores).

The 372 HWEs identified in our three-century study support our contention that windstorms are a high-frequency, chronic-disturbance agent in PNW coastal forests (Fig. 4) as suggested elsewhere (Oregon NHMP, 2006). We found three periods (range: 5–26 years) of elevated storm activity and four periods lacking MSYs (range: 11–27 years) (Fig. 6). The most windstorm-active phase during the 303-year study occurred during 1918–1943 when 30% of all MSYs occurred. MSYs occurred during 14 of the 26 years of this period and included 60% (6 of 10) of the years having ≥4 sites recording HWEs. Windstorm activity before 1918 includes fewer storm clusters and longer intervals without MSYs. The greatest MSY activity in this period occurred during a 5-year episode near the beginning of the 19th century (Fig. 6). More generally, our data show that two thirds of all MSYs occurred following the end of the Little Ice Age circa 1850; the midpoint of our study record (Fig. 6). These results are consistent with post-Little Ice Age changes in climatic conditions (e.g., Mann et al., 1998) that may have been more conducive to the intensification of mid-latitude cyclones.

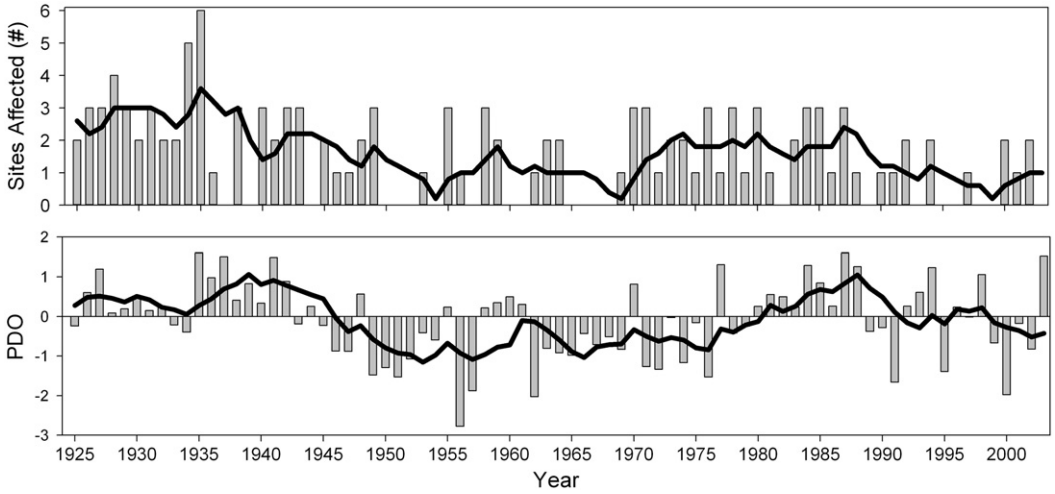

Fig. 5. Number of sites recording a HWE and annual PDO index. Running 5-year means are shown as bold lines.

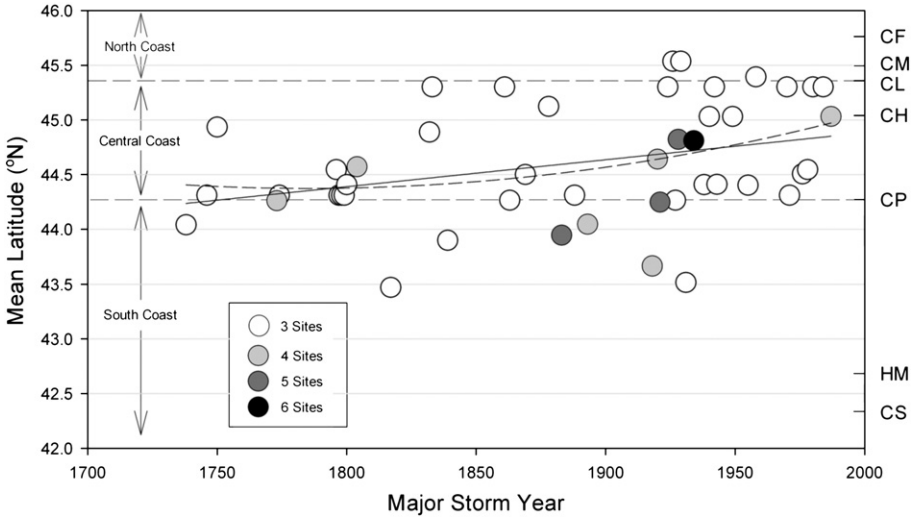

Fig. 6. Mean latitudinal position of 47 Major Storm Years, 1701–2003, with linear trend line ($R^2 = 0.122$., $p = 0.016$ (solid line) and 2nd-order polynomial ($R^2 = 0.137$, $p = 0.039$). The earliest MSY was 1738 and the latest 1987. Circle shading indicates the number of sites affected by a given storm (range: 3–6 sites). Latitudinal position of each of the seven sites is identified on the right y-axis. The MSY of 1985 was omitted from the data set as an outlier.

4.3. PDO–HWE interactions

Based on our results, MSYs appear to correspond to categorical differences in PDO conditions (warm, neutral and cool) as measured by the PDO index. This is supported by two lines of evidence. First, our SEA revealed a significant association between warmer-phase PDO conditions preceding the MSYs identified in the tree-ring record. Second, we found a greater tendency for MSYs to occur during the warm (11 of the 22) and neutral (8 of 34) PDO years recorded between 1925 and 2003. The 19-year warm phase between 1925 and 1943 (mean PDO index of 0.527) was especially notable by its inclusion of 10 MSYs and 15 years (79%) having positive PDO values (Table 2). By contrast, the percentage of MSYs between 1925 and 2003 occurred in only 13% (3 of the 23) of cool PDO years. The period between 1988 and 2003 included fewer HWEs, lacked MSYs, and was characterized by a mean PDO index value of −0.073 with 50% of the years having a negative PDO index value.

The positive association between the PDO and HWEs suggests a change toward increased mid-latitude temperature gradients might promote more favorable conditions for the development of severe mid-latitude cyclones (e.g., Carnell and Senior, 1998). In part, this relationship may be linked to the strengthening of the Aleutian Low that often intensifies during warm PDO phases and are associated with a southerly shift in the storm track (Trenberth and Hurrell, 1994). The synoptic conditions necessary for the development of HWEs are further contingent on these conditions (Mass and Dotson, 2010) including: 1) a large low-pressure cell (e.g., Aleutian Low) developing in the northeastern Pacific Basin with an associated upper-level trough; 2) passage of a short wave through the long-wave trough that occurs during the highest wind period; 3) a strong upper-level (500-hPa) southwesterly flow over the eastern section of the North Pacific; and 4) a strong baroclinic zone created by significant cold (warm) anomalies in the north Pacific (subtropical Pacific). In response to these conditions, Pacific Northwest HWEs tend to track from the southwest toward the northwest following a trajectory consistent with most of the windsnap and blowdown documented in PNW forests (e.g., Ruth and Yoder, 1953).

4.4. ENSO–HWE interactions

Our results failed to show a relationship between SOI conditions and HWE activity. Although similar to PDO conditions, cold SST (La Niña) years were less likely to co-occur with HWEs, a finding contrary to Enloe et al. (2004: 1736) who determined that "gale-force gusts" (i.e., wind speeds > 62.75 kph) increased during ENSO cold phases in the PNW. Whereas El Niño conditions may reinforce the influence of a warm PDO phase on HWE activity, they are not a statistically significant factor associated with HWEs.

4.5. NPI–HWE interactions

NPI conditions, a measure of the strength of the Aleutian Low (D'Arrigo et al., 2005), are also statistically correlated with HWE activity. Annual values of NPI are inversely correlated with HWEs, with elevated HWE activity being associated with the deepening of the Aleutian Low. Oscillations in NPI values are similar to PDO conditions with positive conditions from 1900 to 1924 and 1947 to 1976 and negative conditions from 1925 to 1946 and 1977 to 2003. While we detected a high level of HWE activity during 1925–1946, we did not find the same activity level during the later negative phase, suggesting a deepening of the Aleutian Low is associated with more HWEs, but is a secondary factory to PDO conditions.

4.6. Spatial components

Placing our growth anomaly data within a geographic context revealed a multi-century, northward shift in storm activity. This shift rate varied becoming pronounced in the late 19th century when the mean position of MSYs was characterized by a more northerly geographical component (Table 2). Our results also show the median date for the northernmost five geographic categories (1935) is significantly later ($p < 0.01$, independent-samples median test) than the median date of the remaining 11 more-southerly categories (1869). These findings are consistent with those presented by Mass and Dotson (2010) who noted windstorm activity decreased post-1965 for subregions south of 47° N, but did not report statistical significance.

4.7. Limitations

Despite our success detecting HWEs, not all severe windstorms were identified as MSYs. Four well-documented storms on 9 January 1880 (recorded as HWEs at two sites), 4 December 1951 (no sites), 12 October 1962 (two sites), and 12 December 1995 (no sites) indicate a methodological underestimate of HWE severity of certain events although growth anomalies were recorded at the majority of sites for each storm. Storm-track reconstructions by Read (2011) suggest landfall of

the 1880 and 1951 HWE storms occurred between Newport, Oregon and North Head, Washington before tracking inland (i.e., "Class 2 events"). The tracking and northerly landfall of these storms appears to have spared the majority of our sites from the brunt of the powerful southwesterly winds. Growth anomalies accruing greater than 0% but less than 15% of the total number of cores at each site occurred in 6 (1951) and 5 (1880) of our sites. In these cases, we successfully detected these events but underestimated their severity because of their peripheral and inconsistent offshore and onshore tracking.

Additional factors can further hinder the identification of sub-regional windstorms including pre-existing forest conditions related to earlier windstorms, fire, land use, local topography, or their combination. These factors may have contributed to the weak detection for the 1962 "Columbus Day Storm" (CDS) that is generally recognized as the most severe modern windstorm in the Pacific Northwest (Lynott and Cramer, 1966). Our method detected the CDS storm at six sites (10.5% of all cores) placing it in the 25th percentile—moderate severity— during the 1701–2003 study period. We posit that this moderate ranking is the result of antecedent forest conditions (cf. Teensma et al., 1991; Poage et al., 2009) and local topography (Harcombe et al., 2004); two factors that commonly influence the disturbance severity of windstorms in forest environments. Sub-regional windstorms may also be more difficult to detect using our method because of the few and diminishing number of old-growth forest sites suitable for sampling.

The CDS occurred during a period of forest recovery following the severe 1914–1949 windstorm period and MSYs we identified in 1955 and 1958. Forest clear cuts in conjunction with severe blow down in 1951 also contributed to the pre-CDS era of forest recovery, especially at Cascade Head (Ruth and Yoder, 1953). This storm toppled >2.4 million m^3 of timber along the central and northern Oregon Coast (Ruth and Yoder, 1953) creating widespread young-forest conditions less susceptible to wind-induced tree canopy damage or windfall. The weak tree-growth signal we found might also be related to the widespread clear-cutting along the central Oregon Coast that likely eliminated taller, large-canopy old trees required to document HWEs. Wind-generated forest damage may have been further mitigated by local terrain and the oblique angle of the storm track to much of the coast (Lynott and Cramer, 1966) resulting in sample bias in wind-protected areas on the lee side of higher terrain. Similar to the CDS, our method underrepresented the magnitude of 12 December 1995 windstorm identified by Read (2011) despite its detection at six of our seven sites (7.5% of sampled cores).

Our research represents one of the few regional-scale historical attempts to document windstorms in west-coast climates and is the only study of this type that we are aware of for western North America. It is also the geographically most extensive research to date that identifies and characterizes windstorm histories inferred from tree-ring data. Consequently, this early exploration into regional dendroanemology provides an accurate, albeit conservative 300+ year windstorm history of the Oregon Coast. As such, we identify several challenges that deserve future consideration.

The first among these challenges is obtaining data for a larger geographic perspective examination of mid-latitude windstorms. Oregon represents a small portion of the Pacific Coast of North America and similar HWEs have been documented from northern California (Read, 2011) to Alaska (Mock and Dodds, 2009). A second challenge in developing a more precise history is developing a more complete historical record of these events. The commendable work by Read (2011) is an excellent example of windstorm documentation, yet remains incomplete because of the challenges inherent to the acquisition of early, accurate, local information regarding these events. Nonetheless, four underutilized sources of this information exist in the form of personal diaries (e.g., Knapp and Hadley, 2011), ship logs (e.g., Mock and Dodds, 2009), light house records, and local historical museum archives. Third, we recognize the need to improve our understanding of the confounding influence of storm-track trajectories and to incorporate the historical documentation of antecedent forest conditions and the influence of local terrain and storm landfall location. Fourth, while several coastal, old-growth forest sites suitable for tree-ring research are present in the Pacific Northwest and elsewhere, they are becoming increasingly diminished through attrition related to human-induced and natural disturbance (Van Pelt and Swetnam, 1990; Teensma et al., 1991). The decline of suitable research sites implicates the need for a more concerted effort to increase the number of local- to regional-scale tree-ring studies and the categorical archival of their windstorm-related tree-ring data within the International Tree-Ring Database (ITRDB).

5. Conclusions

Our tree-ring analysis of the timing and distribution of HWEs and major storm years along Oregon's Pacific Coast meets two important objectives. First, it applies a standardized approach to the detection of regional windstorms over a 300+ year period that spans the climate transition between the end of the Little Ice Age and current warmer conditions. Second, our windstorm chronology is sufficiently long to characterize the relationship between windstorms events with annual and decadal climate oscillations and sea-surface pressure. These results provided further evidence that tree-growth anomalies capture the broader context of major storm years and that they accurately match written windstorm accounts documented as early as 1805 in the journals of the Lewis and Clark expedition (Knapp and Hadley, 2011) and the records provided by a variety of historical sources in the late 1800s (Read, 2011). Our results also illustrate the challenges this method provides when dating HWEs. Specifically, the use of tree-growth anomalies appears to underestimate the magnitude and severity of some major windstorms because of physical factors including the influence of storm track trajectories, antecedent forest conditions, topography, an incomplete historical record of HWEs, and the geographic generalization inherent to regional-scale studies. There is also likely some inherent "noise" with using tree-ring data to identify HWEs such as microsite factors, a partial understanding of the physiological response of trees to windstorms, and random events that are a natural part of forest environments. As such, we acknowledge that our findings contain a degree of uncertainty as some major events may not have been fully recorded by the tree-ring data.

Despite these challenges, calibrating proxy data to known conditions and events has important implications regarding the possible effects of increasing SSTs on the magnitude and landfall of mid-latitude cyclones and their associated HWEs. Although continued monitoring of windstorms and their coupling with SSTs will be required to better model the occurrence of HWEs (e.g., Hopkinson et al., 2008), current predictions used to estimate regional PDO conditions (NOAA, 2011) may provide a first step to forecasting PNW windstorms.

Acknowledgments

We thank our research assistants Beth Chappell, Justin Maxwell, Shannon McDonald and Bill Tyminski for their many contributions to this research. The Oregon Department of Parks and Recreation and the US Forest Service kindly granted us access to our research sites. We also thank three anonymous reviewers and the editor for their many insightful and useful comments. Funding for this research was provided by the National Science Foundation (BCS-0750026).

References

Arabas, K.B., Hadley, K.S., Larson, E.R., 2006. Fire history of a naturally fragmented landscape in central Oregon. Canadian Journal of Forest Research 36, 1108–1120.
Biondi, F., Gershunov, A., Cayan, D.R., 2001. North Pacific Decadal climate variability since 1661. Journal of Climate 14, 5–10.
Black, B.A., Abrams, M.D., 2003. Use of boundary-line growth patterns as a basis for dendroecological release criteria. Ecological Applications 13, 1733–1749.

Carnell, R.E., Senior, C.A., 1998. Changes in mid-latitude variability due to increasing greenhouse gases and sulphate aerosols. Climate Dynamics 14, 369–383.
Changnon, S.A., 2009. Temporal and spatial distributions of wind storm damages in the United States. Climatic Change 94, 473–482.
Chen, T.-S., Yoon, J.-H., 2002. Interdecadal variation of the North Pacific wintertime blocking. Monthly Weather Review 130, 3136–3143.
Climate Prediction Center (CPC), 2012. Data available online at: http://www.cpc.ncep.noaa.gov/products/precip/CWlink/pna/norm.pna.monthly.b5001.current.ascii.table.
Cook, E.R., 2005. A time series analysis approach to tree-ring standardization. Dissertation, University of Arizona, Tucson. 171 pp.
Cook, E.R., Holmes, R.L., 1986. Program ARSTAN User's Manual. Laboratory of Tree-Ring Research, University of Arizona, Tucson.
D'Arrigo, R., Villalba, R., Wiles, G., 2001. Tree-ring estimates of Pacific climate variability. Climate Dynamics 18, 219–224.
D'Arrigo, R., Wilson, R., Deser, C., Wiles, G., Cook, E., 2005. Tropic-North Pacific climate linkages over the past four centuries. Journal of Climate 18, 5253–5265.
Decker, F., Cramer, O., Harper, B., 1962. The Columbus Day 'Big Blow' in Oregon. Weatherwise 16, 238–245.
Donnelly, J.P., Woodruff, J.D., 2007. Intense hurricane activity over the past 5,000 years controlled by El Niño and the West African Monsoon. Nature 447, 465–468.
Donnelly, J.P., Roll, S., Wengren, M., Butler, J., Lederer, R., Webb III, T., 2001. Sedimentary evidence of intense hurricane strikes from New Jersey. Geology 29, 615–618.
Enloe, J., O'Brien, J.J., Smith, S.R., 2004. ENSO impacts on peak wind gusts in the United States. Journal of Climate 17, 1728–1737.
Franklin, J.F., Spies, T.A., Van Pelt, R., Carey, A.B., Throngurgh, D.A., Berg, D.R., Lindenmayer, D.B., Harmon, M.E., Keeton, W.S., Shaw, D.C., Bible, K., Chen, J., 2002. Disturbances and structural development of natural forest ecosystems with silvicultural implications, using Douglas-fir forests as an example. Forest Ecology and Management 155, 399–423.
Garrett, C., Petrie, B., 1981. Dynamical aspects of the flow through the Strait of Belle Isle. Journal of Physical Oceanography 11, 376–393.
Gedalof, Z., Smith, D.J., 2001. Interdecadal climate variability and regime-scale shifts in Pacific North America. Geophysical Research Letters 28, 1515–1518.
Grissino-Mayer, H.D., 2001. Evaluating crossdating accuracy: a manual and tutorial for the computer program COFECHA. Tree-Ring Research 57, 205–221.
Grissino-Mayer, H.D., Swetnam, T.W., 2000. Century-scale climate forcing of fire regimes in the American Southwest. The Holocene 10, 213–220.
Hadley, K.S., Knapp, P.A., 2011. Detection of high-wind events using tree-ring data. Canadian Journal of Forest Research 41, 1121–1129.
Harcombe, P.A., Greene, S.E., Kramer, M.G., Ackers, S.A., Spies, T.A., Valentine, T., 2004. The influence of fire and windthrow dynamics on a coastal spruce-hemlock forest in Oregon, USA, based on aerial photographs spanning 40 years. Forest Ecology and Management 194, 71–82.
Harris, A.S., 1990. Picea sitchensis. In: Burns, R.M., Honkala, B.H. (Eds.), Silvics of North America, Vol. 1, Conifers. Forest Service Agriculture Handbook, 654. U.S.D.A., Washington DC. http://www.na.fs.fed.us/spfo/pubs/silvics_manual/table_of_contents.htm.
Heyerdahl, E.K., Brubaker, L.B., Agee, J.K., 2002. Annual and decadal climate forcing of historical fire regimes in the interior Pacific Northwest, USA. The Holocene 12, 597–604.
Holmes, R.L., 1983. Computer-assisted quality control in tree-ring dating and measurement. Tree-Ring Bulletin 43, 69–78.
Hopkinson, C.S., Lugo, A.E., Alber, M., Covich, A.P., Van Bloem, S.J., 2008. Forecasting effects of sea-level rise and windstorms on coastal and inland ecosystems. Frontiers in Ecology and the Environment 6, 255–263.
Keim, B.D., Muller, R.A., Stone, G., 2007. Spatiotemporal patterns of and return periods of tropical storm and hurricane strikes from Maine to Texas. Journal of Climate 20, 3498–3509.
Kirk, R., Franklin, J., 1992. The Olympic Rain Forest. University of Washington Press. 128 pp.
Knapp, P.A., Hadley, K.S., 2011. Lewis and Clarks' tempest: the "Perfect Storm" of November 1805. The Holocene 21, 693–697.
Liu, K.-b., Fearn, M.L., 1993. Lake sediment record of late Holocene hurricane activities from coastal Alabama. Geology 21, 793–796.
Liu, K.-b., Fearn, M.L., 2000. Reconstruction of prehistoric landfall frequencies of catastrophic hurricanes in northwestern Florida from lake sediment records. Quaternary Research 54, 238–245.
Lynott, R.E., Cramer, O.P., 1966. Detailed analysis of the 1962 Columbus Day windstorm in Oregon and Washington. Monthly Weather Review 94, 105–117.
MacDonald, G.M., Case, R.A., 2005. Variations in the Pacific Decadal Oscillation over the past millennium. Geophysical Research Letters 32, L08703, http://dx.doi.org/10.1029/2005GL022478.
Mann, M.E., Bradley, R.S., Hughes, M.K., 1998. Global-scale temperature patterns and climate forcing over the past six centuries. Nature 392, 779–787.
Mantua, N.J., Hare, S.R., Zhang, Y., Wallace, J.M., Francis, R.C., 1997. A Pacific interdecadal climate oscillation with impacts on salmon production. Bulletin of the American Meteorological Society 78, 1069–1079.
Mass, C., Dotson, B., 2010. Major extratropical cyclones of the Northwest United States: historical review, climatology, and synoptic environment. Monthly Weather Review 138, 2499–2528.
Mock, C.J., Dodds, S.F., 2009. The Sitka Hurricane of October 1880. In: Dupigny-Giroux, L.-A., Mock, C.J. (Eds.), Historical Climate Variability and Impacts in North America Springer-Science and Business Media, pp. 99–106.
MWR, 1894, 1914–1949. Condensed climatological summary (for months of October through April). Monthly Weather Review 41–77 (various pages).
NCDC, 2010. Monthly climatic data for Oregon Division 1 Available online at: http://www7.ncdc.noaa.gov/CDO/CDODivisionalSelect.jsp#2010Accessed October 21.
NOAA, 2011. Climate Prediction CenterAvailable online at: http://www.cpc.ncep.noaa.gov/products/predictions/90day/fxus05.html2011[accessed 18 February 2011].
Nyberg, J., Malmgren, B.A., Winter, A., Jury, M.R., Kilbourne, K.H., Quinn, T.M., 2007. Low Atlantic hurricane activity in the 1970s and 1980s compared to the past 270 years. Nature 447, 698–701.
Oregon Natural Hazard Mitigation Plan, 2006. Available at: http://csc.uoregon.edu/opdr/sites/csc.uoregon.edu.opdr/files/OR-NHMP_wind_chapter_2009.pdf2006.
Poage, N.J., Weisberg, P.J., Impara, P.C., Tappeiner, J.C., Sensenig, T.S., 2009. Influences of climate, fire, and topography on contemporary age structure patterns of Douglas-fir at 205 old forest sites in western Oregon. Canadian Journal of Forest Research 39, 1518–1530.
Read, W., 2011. The Storm King. Some historical weather events in the Pacific Northwest Available online at: http://www.climate.washington.edu/stormking/2011[accessed 10 January 2011].
Redmond, K.T., Koch, R.W., 1991. Surface climate and streamflow variability in the western United States and their relationship to large-scale circulation indices. Water Resources Research 27, 2381–2399.
Reed, R.J., 1980. Destructive winds caused by an orographically induced mesoscale cyclone. Bulletin of the American Meteorological Society 61, 1346–1355.
Reed, R.J., Albright, M.D., 1986. A case study of explosive cyclogenesis in the eastern Pacific. Monthly Weather Review 114, 2297–2319.
Ruth, R.H., Yoder, R.A., 1953. Reducing wind damage in the forests of the Oregon Coast Range. USFS, PNW - Research Paper, 7. 30 pp.
Speer, J.H., 2010. Fundamentals of Tree-Ring Research. University of Arizona Press. 368 pp.
Speer, J.H., Swetnam, T.W., Wickman, B.E., Youngblood, A., 2001. Changes in pandora moth outbreak dynamics during the past 622 years. Ecology 82, 679–697.
Stokes, M.A., Smiley, T.L., 1968. An Introduction to Tree-Ring Dating. University of Chicago Press, Chicago. 73 pp.
Teensma, P.D.A., Rienstra, J.T., Yeiter, M.A., 1991. Preliminary reconstruction and analysis of change in forest stand age classes of the Oregon Coast Range from 1850 to 1890. USDI Bureau of Land Management Technical Note T/N OR-9. .
Trenberth, K.E., Hurrell, J.W., 1994. Decadal atmosphere–ocean variations in the Pacific. Climate Dynamics 9, 303–319 (Data available online at: http://www.cgd.ucar.edu/cas/jhurrell/npindex.html).
Van Pelt, N.S., Swetnam, T.W., 1990. Conservation and stewardship of tree-ring resources: living trees and subfossil wood. Natural Areas Journal 10, 19–27.
Waring, R.H., Franklin, J.F., 1979. Evergreen coniferous forests of the Pacific Northwest. Science 204, 1380–1386.
Weidman, R.H., 1920. The windfall problem in the Klamath Region. Oregon. Journal of Forestry 18, 837–843.
Weisberg, P.J., Swanson, F.J., 2003. Regional synchroneity in fire regimes of western Oregon and Washington, USA. Forest Ecology and Management 172, 17–28.
WRCC, 2010. Western Regional Climate Center, classification of El Niño and La Niña winters Available online at: http://wrcc.dri.edu/enso/ensodef.html [accessed 1 November 2010].
Yamaguchi, D.K., 1991. A simple method for cross-dating increment cores from living trees. Canadian Journal of Forest Research 21, 414–416.
Zar, J.H., 1999. Biostatistical Analysis, 4th ed. Prentice-Hall, Upper Saddle River, New Jersey. 929 pp.